NeuroToxicology 52 (2016) 89–97

Contents lists available at ScienceDirect

NeuroToxicology

Full Length Article

Methylmercury upregulates RE-1 silencing transcription factor (REST) in SH-SY5Y cells and mouse cerebellum

Natascia Guida [a], Giusy Laudati [b], Serenella Anzilotti [a], Rossana Sirabella [b], Ornella Cuomo [b], Paola Brancaccio [b], Marianna Santopaolo [c], Mario Galgani [d], Paolo Montuori [e], Gianfranco Di Renzo [b], Lorella M.T Canzoniero [b,f], Luigi Formisano [b,f,*]

[a] IRCSS SDN, Naples 80131, Italy
[b] Division of Pharmacology, Department of Neuroscience, Reproductive and Dentistry Sciences, School of Medicine, "Federico II" University of Naples, Naples 80131, Italy
[c] Dipartimento di Medicina Molecolare e Biotecnologie Mediche, Università degli Studi di Napoli "Federico II" Napoli, 80131, Italy
[d] Laboratorio di Immunologia, Istituto di Endocrinologia e Oncologia Sperimentale, Consiglio Nazionale delle Ricerche (IEOS-CNR), Napoli, 80131, Italy
[e] Department of Preventive Medical Sciences, University Federico II, Via Pansini 5, 80131 Naples, Italy
[f] Division of Pharmacology, Department of Science and Technology, University of Sannio, 82100 Benevento, Italy

ARTICLE INFO

Article history:
Received 31 July 2015
Received in revised form 9 November 2015
Accepted 11 November 2015
Available online 21 November 2015

Keywords:
Methylmercury
REST
Acetylation
Cerebellum

ABSTRACT

Methylmercury (MeHg) is a highly neurotoxic compound that, in adequate doses, can cause damage to the brain, including developmental defects and in severe cases cell death. The RE-1–silencing transcription factor (REST) has been found to be involved in the neurotoxic effects of environmental pollutants such as polychlorinated biphenyls (PCBs). In this study, we investigated the effects of MeHg treatment on REST expression and its role in MeHg-induced neurotoxicity in neuroblastoma SH-SY5Y cells. We found that MeHg exposure caused a dose- and time- dependent apoptotic cell death, as evidenced by the appearance of apoptotic hallmarks including caspase-3 processing and annexin V uptake. Moreover, MeHg increased REST gene and gene product expression. MeHg-induced apoptotic cell death was completely abolished by REST knockdown. Interestingly, MeHg (1 μM/24 h) increased the expression of REST Corepressor (Co-REST) and its binding with REST whereas the other REST cofactor mammalian SIN3 homolog A transcription regulator (mSin3A) was not modified. In addition, we demonstrated that the acetylation of histone protein H4 was reduced after MeHg treatment and was critical for MeHg-induced apoptosis.

Accordingly, the pan-histone deacetylase inhibitor trichostatin-A (TSA) prevented MeHg-induced histone protein H4 deacetylation, thereby reverting MeHg-induced neurotoxic effect. Male mice subcutaneously injected with 10 mg/kg of MeHg for 10 days showed an increase in REST expression in the granule cell layer of the cerebellum together with a decrease in histone H4 acetylation. Collectively, we demonstrated that methylmercury exposure can cause neurotoxicity by activating REST gene expression and H4 deacetylation.

1. Introduction

The ubiquitous environmental neurotoxin methylmercury (MeHg) readily crosses the blood-brain barrier, through the L-type large neutral amino acid transporter, and induces serious neurological damage (Simmons-Willis et al., 2002). Low concentrations of mercury are able to induce oxidative stress, cell cytotoxicity and to increase the secretion of β-amyloid 1–40 and 1–42, which may lead to neurodegenerative diseases, such as Alzheimer's and Parkinson's diseases (Olivieri et al., 2002). Moreover, an increase of hypoesthesia, ataxia, dysarthria and impairment of hearing and visual change (Ninomiya et al., 1995) has been found in the patients 10 years after the end of methylmercury dispersion from Minamata, on coast of Shiranui sea, as a consequence of a long-term exposure study to low doses. Indeed, observational studies of individuals exposed to high levels of neurotoxin early in life in Minamata, where methylmercury was discharged in waste water showed neurological dysfunction such as cerebellar ataxia, visual

* Corresponding author at: Division of Pharmacology, Department of Science and Technology, University of Sannio, Via Port' Arsa 11, 82100 Benevento, Italy. Tel.: +39 0824305116/0817463315; fax: +39 0824305142.
E-mail address: cformisa@unisannio.it (L. Formisano).

http://dx.doi.org/10.1016/j.neuro.2015.11.007
0161-813X/

impairment, weakness of extremities, and sensory disturbances (Eto et al., 2010). The brain regions most susceptible to MeHg-mediated injury are the brain cortex and the cerebellum (Fahrion et al., 2012). For the cerebellum, the degeneration seems to occur particularly in cerebellar granule cells (CGCs) (Fujimura and Usuki, 2014, 2015). Interestingly, in experimental animal studies MeHg induces degeneration of the cerebellar cortex, leaving Purkinje cells intact (Fujimura and Usuki, 2014, 2015, Nagashima et al., 1996). Different molecular targets have been associated with MeHg-induced neuronal cell death, including the N-methyl-D-aspartate (NMDA) receptors (Ndountse and Chan, 2008), Ca^{2+} channels (Gasso et al., 2001), Rho-associated coiled coil-forming protein kinase (ROCK) (Fujimura et al., 2011), and, recently, the suppression of tropomyosin receptor kinase A (TrkA) pathway (Fujimura and Usuki, 2015).

A new interesting target to investigate in MeHg-induced toxicity is the repressor element 1 (RE-1)–silencing transcription factor (REST). Indeed, perturbation in the expression and function of REST is involved in several neurological disorder such as stroke (Formisano et al., 2015b, Formisano et al., 2013), epilepsy (McClelland et al., 2014), Huntington disease (Zuccato et al., 2003), neuropathic pain (Uchida et al., 2010), and neurotoxicity induced by the environmental neurotoxicants PCBs (Formisano et al., 2011, Formisano et al., 2014, Formisano et al., 2015a). It is well known that REST, by binding to the RE-1 elements, actively represses a large array of coding and non coding RNAs, such as miR-132, all of which have a pivotal role in synaptogenesis, synaptic plasticity, and structural remodeling (Hwang et al., 2014). Thus, in brain ischemia REST translocates in the nucleus, thus repressing some target genes, such as α-amino-3-hydroxy-5-methyl-4-isoxazole-propionic acid receptor (AMPAR) "Ca^{2+} ion gatekeeper" subunit GluR2 and sodium-calcium exchanger 1 (NCX1). REST induces its toxic effect through histone deacetylation (Formisano et al., 2013, Noh et al., 2012). Indeed, treatment with the pan-histone deacetylase (HDAC) inhibitor trichostatin-A (TSA) or the HDAC class I inhibitor MS-275 rescues neurons from REST-induced cell death (Formisano et al., 2015b, Noh et al., 2012).

Since we hypothesized the involvement of REST in methylmercury-induced neurotoxicity, we examined the effects of MeHg treatment on REST expression and its role in MeHg-induced neurotoxicity in neuroblastoma SH-SY5Y cells and in mouse cerebellum. Our *in vitro* analyses revealed that REST and histone H4 protein deacetylation are involved in MeHg-induced neurotoxicity; consistently, our *in vivo* experiments indicate that the subcutaneous administration of MeHg (10 mg/Kg/day) in mice leads to increased levels of REST protein expression in the cerebellum, a region highly vulnerable to MeHg-induced neurotoxicity.

2. Material and methods

2.1. Drug and chemicals

Methylmercury (II) chloride (MeHg) (cod: 442534 stock solution 100 μM) and trichostatin A (TSA) (cod: T8552 stock solution 100 μM) both obtained from Sigma–Aldrich (St. Louis, MO) were dissolved in water with NaHCO3 at 25 mM (Zimmermann et al., 2014), and with dimethyl sulfoxide (DMSO), respectively. Culture media and sera were purchased from Invitrogen (Milan, Italy). For *in vivo* experiments, MeHg was coniugated with cysteine (Cys) and its reaction was confirmed by Ellman's reaction (Zimmermann et al., 2014). All chemicals were diluted in cell culture medium. In all experiments, the control group (CTL) was treated with vehicle: water with NaHCO3 (25 nM) for MeHg and DMSO (0.1%) for TSA.

2.2. Cell Cultures and siRNA transfections

Human neuroblastoma SH-SY5Y cells (IRCCS Azienda Ospedaliera Universitaria San Martino-IST-Instituto Nazionale per la Ricerca sul Cancro, Genoa, Italy) were grown as previously described (Formisano et al., 2014). After 24 h of cell seeding, MeHg at 0.1–3 μM was added to Dulbecco's Modified Eagle Medium (DMEM) medium containing 1% fetal bovine serum (FBS) for 6–36 h. After cell seeding and before MeHg exposure (1 μM/24 h), cells were pre-treated with TSA (10–50 nM) for 2 h. For REST synthetic small interfering RNA (siRNA) transfection, cells were transfected with siRNA against REST (siREST) and negative control siRNA (siCTL) 24 h before MeHg treatment (1 μM/24 h). The transfection was performed with HiPerFect Transfection Reagent (Quiagen) in accordance with the manufacturer's protocol. siREST (20 nM) was transfected into SH-SY5Y cells as previously reported (Formisano et al., 2015a). The sequences of siRNA for REST were as follows: forward 5′-GAUGGAGGGUGCCCAGAUATT-3′ and reverse 5′-UAUCUGGGCACCCUCCAUCTG-3′ (NM_005612). For siCTL All Stars Negative Control siRNA (Qiagen) (cod: 1027280) was used. siRNA transfection efficiency was 60% for SH-SY5Y (data not shown). Finally, cells were exposed to MeHg (1 μM) for 24 h. They were then plated in 24-multiwell plates at a density of 2×10^5 for the MTT assay, annexin V- and propidium iodide staining, and in 100 mm well plates at a density of 10×10^5 for quantitative reverse-transcription polymerase chain reaction (RT-PCR), Western blot, and immunoprecipitation analyses.

2.3. Determination of cell viability

Cell viability was evaluated by MTT assay (Guida et al., 2014) under various experimental conditions: (1) cells were treated with MeHg at increasing concentrations of 0.1–3 μM for 24 h; (2) cells were treated with MeHg at 1 μM for 6–36 h; (3) cells were transfected with siREST and siCTL or pre-treated with TSA (10–50 nM) for 2 h, and, after 24 h, they further incubated with 1 μM MeHg for 24 h.

2.4. Annexin V/Propidium iodide staining

Experiments were performed as previously reported (Formisano et al., 2015a, Guida et al., 2014). Briefly, cells were treated with MeHg either at 0.1–3 μM for 24 h or at 1 μM for 6–36 h. In other experiments, cells were transfected with siREST and siCTL and, 24 h later, treated with 1 μM MeHg for 24 h. After MeHg exposure, they were washed with ice-cold PBS and collected on ice. Apoptosis and necrosis were evaluated by staining the cells with annexin V and propidium iodide (PI), respectively, for 30 min in ice-cold PBS containing both dyes and after that, they were suspended for deposition on slides. A negative sample was acquired for control staining. The analysis was performed on 10 fields for each experimental condition. In addition, the cells were at a concentration of 150,000/ml, and the analyses were performed on 35,000 cells for each experimental condition.

2.5. Quantitative reverse transcription polymerase chain reaction (qRT-PCR) analysis

Total RNA extraction and cDNA synthesis from SH-SY5Y cells and quantitative real-time PCR were performed as previously reported (Formisano et al., 2015a, Guida et al., 2014). Samples were amplified simultaneously in quadruplicate in a one-assay run, and the threshold cycle (cT) value for each experimental group was determined. Normalization of the data was performed using ribosomal protein L19 (L19). To evaluate differences in mRNA content between groups, normalized values were entered into the

formula $2^{-\Delta\Delta ct}$. The oligonucleotide sequences for REST and L19 were as follows: The oligonucleotide sequences were for REST: 5′-TCACATGGAGCCAATTTCCA-3′ and 5′-TTTCCTTTGGCAGTGGTGGT-3′ (XM_011534402.1); and for L19:5′-CTAGTGTCCTCCGCTGTGG-3′ and 5′- AAGGTGTTTTTCCGGCATC-3′ (NM_032019.5) (Formisano et al., 2011, Guida et al., 2014).

2.6. Western Blot analysis and Immunoprecipitation

Total protein extracts from cells and brain tissues (mice cerebellum and cortex) were performed as previously reported (Formisano et al., 2013). In brief, 100 μg of proteins was used to detect REST, CoREST, and mSIN3A, whereas 50 μg was used for histone H4 acetylation. Proteins from cells and tissues were separated on an 8% SDS-PAGE for REST, CoREST, and mSIN3A, and on 15% SDS-PAGE for histone H4 acetylation. After that, running proteins were electroblotted on nitrocellulose (Ge Healthcare, Milan, IT). Immunoprecipitation of REST in MeHg-treated cells was performed as previously described (Formisano et al., 2015a). In brief, cell lysates (1 mg) were immunoprecipitated overnight at 4 °C using REST antibody (3 μg) and IgG as a negative control. Protein A/G-agarose beads (25 μl) (sc-2003 Santa Cruz Biotechnology) were used to precipitate the bound protein. The precipitated samples were then subjected to Western blot analysis. The antibodies used were: anti-calpain (sc-30064, Santa Cruz Biotechnology, 1:500), anti-CoREST (07-455, Millipore, 1:1000), anti-histone H4 acetylated (05-858, Millipore, 1:1000), mSin3A (sc-994, Santa Cruz Biotechnology, 1:1000), anti-caspase-3 (sc-7272, Santa Cruz Biotechnology, 1:500), anti-REST (07-579, Millipore, 1:1000) and anti-Tubulin (T5168, Sigma-Aldrich, 1:10000) (Guida et al., 2014).

2.7. In vivo *studies*

2.7.1. Experimental groups

Adult male mice C57/BL6 (90 days old, weight 50 g) (Charles River) were housed under diurnal lighting conditions (12 h darkness/light). Experiments were performed according to the international guidelines for care and use of experimental animals of the European Community Council directive (86/609/EEC). All experiments were approved by the Institutional Animal Care and Use Committee of "Federico II" University of Naples, IT.

2.7.2. Immunohistochemistry (IHS)

MeHg-Cys complex (10 mg/Kg) was dissolved in water with NaHCO3 at 25 mM and was subcutaneously administered to mice (2 ml/Kg) once a day for 10 days (Zimmermann et al., 2014). Animals were divided into two groups of 5 animals: one group, the control (CTL), received water with NaHCO3 at 25 mM and the other group, MeHg, received the MeHg-Cys complex. After 10 days, both animal groups were anesthetized intraperitoneally with chloral hydrate (300 mg/kg) and a transcardiac perfusion was made with 4% (wt/vol) paraformaldehyde (PFA) in phosphate buffer (PBS). Serial 10-μm-thick sections were cut in a cryostat and incubated overnight in anti-REST and anti-H4 acetyl antibodies, diluted in PBS 2% bovine serum albumin (BSA), and 0.1% Triton X-100. Afterward, the slices were incubated in a mixture of fluorescent-labeled secondary antibodies (Alexa 488 or – Alexa 568-conjugated IgG, 1:200; Molecular Probes, Eugene, OR). Images were observed with a Zeiss LSM 510 META Laser-Scanning Confocal Microscope.

2.8. Statistical analysis

Data are expressed as the mean ± S.E.M. Statistical comparisons between the experimental groups were performed using one-way analysis of variance followed by the Newman-Keuls test. $P < 0.05$ was considered statistically significant.

3. Results

3.1. MeHg exposure induces apoptotic cell death by increasing REST expression in SH-SY5Y cells

When SH-SY5Y cells were exposed to different concentrations of MeHg (0.1–3 μM) for 24 h, a dose-related reduction of cell viability was detected by the MTT assay (Fig. 1A). Furthermore, cell death was evaluated with FITC-conjugated annexin V, a marker of apoptosis (Martin et al., 1995) and with propidum iodide (PI), a marker of necrosis (Bal-Price and Brown, 2000); it was finally analyzed with a Tali™ Image Cytometer. Following 24 h of MeHg treatment at 0.1–3 μM, cells were significantly positive for annexin V, but not for PI (Fig. 1B and C). Notably, incubation (6-36 h) with MeHg at 1 μM induced a time-dependent decrease in cell viability and an increase in annexin V-positive cells. However, it did not modify the number of PI-positive cells (Fig. 1 E-G).

Since 1 μM MeHg treatment for 24 h damaged approximately 50% of cells, this concentration and this time point were chosen for our experiments. Interestingly, appearance of active Caspase 3 with MeHg exposure was seen, as opposed to control cells (Fig. 1D); however, the necrotic marker calpain was unaffected (Fig. 1H). Regarding the effect of MeHg exposure on REST expression, MeHg (1 μM) strongly increased REST mRNA and protein expression (Fig. 2A and B).

Next the role of REST in MeHg-induced cell death was investigated. To this aim, REST was knocked down by specific siRNA transfection (siREST). As shown in Fig. 2C, siREST significantly reduced REST expression by 65% compared to siCTL. Importantly, REST knockdown reverted not only MeHg-induced cleavage of caspase-3 (Fig. 2D), but also MeHg toxicity, as revealed by MTT assay and by annexin V uptake (Fig. 2E and F). However, it had no effect on PI staining (data not shown).

3.2. MeHg induces the formation of REST/Co-REST complex in SH-SY5Y cells

REST-dependent gene silencing requires the action of transcriptional co-repressors, two of which are mSIN3A and CoREST (Levenson and Sweatt, 2005). As shown in Fig. 2A–C, MeHg (1 μM/24 h) increased the expression of Co-REST, but not of mSIN3A, while simultaneously reducing histone H4 acetylation. Next, total proteins from cells treated with MeHg were immunoprecipitated with REST antibody and the immunoprecipitate was immunoblotted with antibodies for CoREST or mSin3A. After 24 h of treatment with MeHg (1 μM), REST interacted with CoREST, but not with mSIN3A, whereas no interaction was detected in the preimmune (PI) group (Fig. 3D and E).

3.3. TSA prevents MeHg-induced cell death by blocking histone protein H4 deacetylation

It is well known that REST exerts its neurotoxic effect by epigenetic mechanisms, such as histone deacetylation (Kazantsev and Thompson, 2008). To this aim, the cells were pre-treated with the pan-histone HDAC inhibitor TSA at 10, 25, and 50 nM. Not only did TSA cause a remarkable dose-dependent protective effect against MeHg-induced cell death (1 μM/24 h), as revealed by MTT (Fig. 1A), but it also counteracted MeHg-induced cleavage of caspase-3 (Fig. 4D). Furthermore, Western Blot experiments showed that whereas MeHg decreased histone H4 acetylation, TSA blocked this reduction (Fig. 4 E).

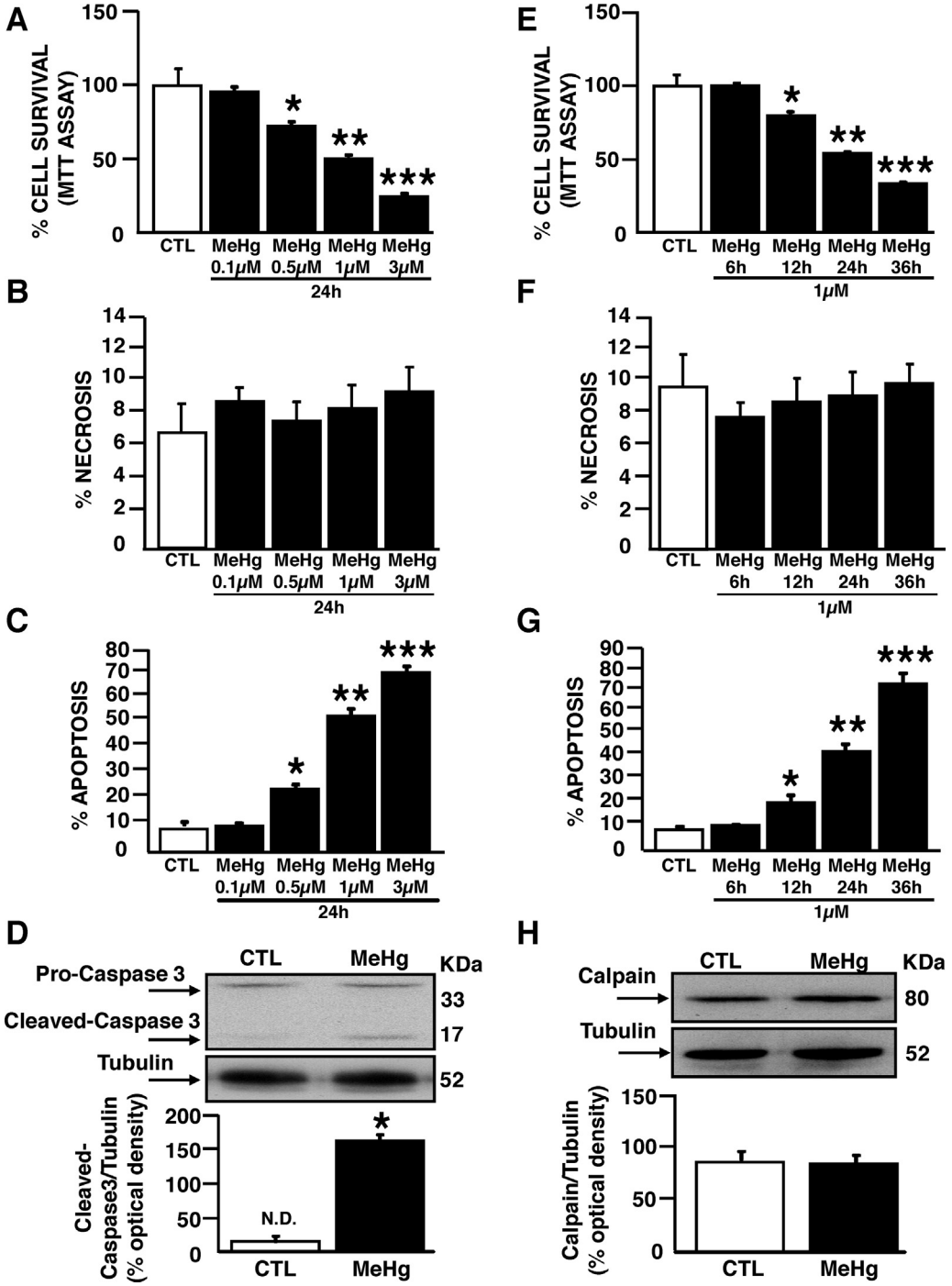

Fig. 1. Effect of MeHg on SH-SY5Y cell survival.
(A–C) Effect of 24 h of MeHg (0.1, 0.5, 1, and 3 μM) exposure on mitochondrial activity (MTT), necrosis (PI uptake) and apoptosis (Annexin V uptake). Bars represent mean ± S.E.M. obtained from four independent experimental sessions. $^{*}P < 0.05$ vs. CTL and 0.1 μM, $^{**}P < 0.05$ vs. CTL,0.1 and 0.5 μM; $^{***}P < 0.05$ vs. all. (E-G) Effect of 1 μM MeHg exposure on MTT, necrosis (PI uptake) and apoptosis (Annexin V uptake) and at 6, 12, 24 and 36 h. Bars represent mean ± S.E.M. obtained from four independent experimental sessions. $^{*}P < 0.05$ vs. CTL and 6 h, $^{**}P < 0.05$ vs. CTL, 6 h and 12 h; $^{***}P < 0.05$ vs. (D, H) Western blots of pro-caspase-3, cleaved caspase-3, and calpain protein levels in CTL after 24 h of MeHg (1 μM). Graphs show the quantification of the ratio of cleaved caspase-3 or calpain to tubulin. Bars represent mean ± S.E.M. obtained from three independent experiments. $^{*}P < 0.05$ vs CTL, and N.D. not detectable.

3.4. MeHg increases REST and decreases histone H4 acetylation in mouse cerebellum brain

In vivo models of MeHg neurotoxicity were investigated to further validate our in vitro results. Accordingly, REST and histone H4 acetylation expression was evaluated in the cortex and cerebellum of mice subcutaneously-injected with MeHg (10 mg/Kg) for 10 days. Importantly, a MeHg-Cys complex was administered to raise MeHg accumulation in the brain (Roos et al., 2011). The time point and the dose of exposure used in this study were the same as those already known to induce significant motor impairments and accumulation in the brain, especially in the cerebellum (Zimmermann et al., 2014). Consistently, we observed severe locomotor deficits in MeHg-treated mice similar to those already described (Zimmermann et al., 2014)

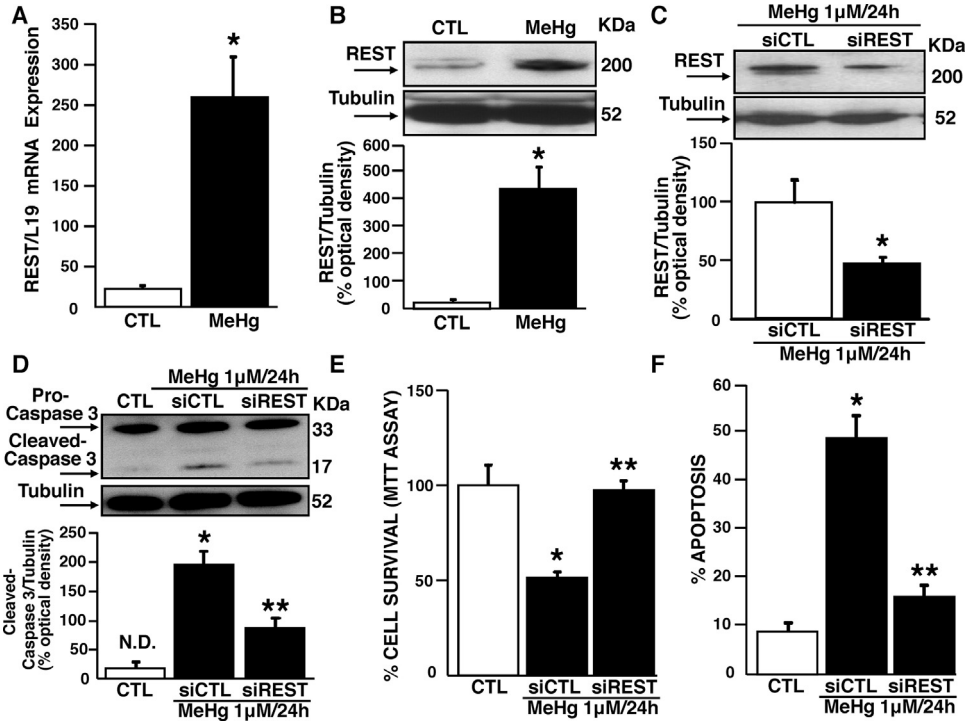

Fig. 2. Effect of MeHg on the levels of REST mRNA and protein expression and of siREST on MeHg-induced apoptotic cell death.
(A,B) qRT-PCR and representative Western blot of REST and protein treated for 24 h with MeHg (1 μM) or under control conditions (CTL). Graphs show quantification of ratio of REST to tubulin for Western Blot experiments and of REST to L19 for qRT-PCR experiments. Bars represent mean ± S.E.M. obtained from three independent experiments for Western Blot and four independent experiments for qRT-PCR. $^{*}P < 0.05$ vs CTL. (C) Representative Western blot and quantification of REST protein expression in SH-SY5Y cells treated for 24 h with MeHg 1 μM and transfected with siCTL and siREST in. Graphs show quantification of the ratio of REST to tubulin. Bars represent mean ± S.E.M. obtained from three independent experiments. $^{*}P < 0.05$ vs siCTL. (D) Representative Western blots of pro-caspase-3, cleaved caspase-3, and tubulin levels in CTL or after a 24 h exposure to 1 μM MeHg alone or after siREST transfection. Graphs show quantification of the ratio of cleaved caspase-3 to tubulin. Bars represent mean ± S.E.M. obtained from four independent experimental sessions. $^{*}P < 0.05$ vs CTL $^{**}P < 0.05$ vs MeHg 1 μM/24 h and N.D. not detectable. (E,F) Effect of a 24-h exposure to 1 μM MeHg alone or after siREST transfection on MTT and apoptosis (Annexin V uptake) Bars represent mean ± S.E.M. obtained from four independent experimental sessions. $^{*}P < 0.05$ vs. CTL and $^{**}P < 0.05$ vs. 1 μM MeHg.

(data not shown). An increase in REST protein expression and a decrease in acetylation of histone protein H4 were detected in the cerebellum (Fig. 5A,B), but not in the cortex (Fig. 5C,D) of the MeHg-treated animals, compared with the vehicle-treated group (CTL).

The relationship between REST and acetylated histone H4 expression in the cerebellum of mice treated with MeHg was further explored by performing IHS analysis by confocal microscopy. REST was basally expressed in the granular layer (GL), in Purkinje cells (PC), and in the molecular layer (ML), whereas acetylated histone H4 was highly expressed in GL (Fig. 5E,F) but dimly expressed in PC and ML (Fig. 5G,H). Following 10 days of MeHg administration, REST expression strongly increased in GL, as evidenced by the intense REST immunosignal in the cells of this region (Fig. 5I, L). By contrast, H4 acetylation immunosignal decreased in the same region (Fig. 5M, N). These results validate our *in vitro* findings and suggest that environmental exposure to MeHg increases REST expression and deacetylation of histone H4 in the cerebellum granular cell layer.

4. Discussion

In the present study we showed that MeHg induces a dose- and time-dependent reduction in cell viability in SH-SY5Y cells. Interestingly, MeHg-induced reduction of cell viability was accompanied by an increase in cleaved caspase-3 and in annexin V uptake, but not in calpain and in PI uptake. These findings suggest that cell death is due to the activation of an apoptotic but not of a necrotic pathway. In addition, whereas MeHg induced an increase in REST mRNA and protein expression, siRNA against REST prevented MeHg-induced apoptotic cell death. To our knowledge, this is the first evidence showing that REST is involved in the neurodetrimental effects of MeHg. This evidence is in accordance with the known pro-death role played by REST in brain ischemia, where it increases in the nuclei of CA1 hippocampal neurons (Formisano et al., 2007, Kaneko et al., 2014, Noh et al., 2012) and in the cortex (Formisano et al., 2015b, Formisano et al., 2013). Likewise, REST also seems to be involved in the toxic effect exerted by other environmental neurotoxins like PCBs. Indeed, evidence of REST involvement in PCB neurotoxicity is that whereas its mRNA levels and protein expression are induced after PCB exposure, REST knockdown blocks A1254 PCB mixture-induced cell death in SH-SY5Y cells and cortical neurons (Formisano et al., 2011, Formisano et al., 2014, Formisano et al., 2015b).

Although REST is fully involved in both PCBs and MeHg toxic effects, the mechanisms whereby it actually contributes to neurotoxicity following exposure to both toxicants do seem to differ. For instance, during A1254 exposure, REST induces necrotic cell death (Formisano et al., 2015a). Instead, in this study we found that after MeHg exposure REST knockdown reverted annexin V uptake and cleavage of caspase 3, a finding triggered after exposure to MeHg, demonstrating that this toxicant induces apoptosis by increasing REST expression. These results are in accordance with other authors showing that MeHg determines cell death by activating an apoptotic mechanism (Fujimura and Usuki, 2015, Ndountse and Chan, 2008).

It is well known that REST recruits mSin3A at the N-terminal (Huang et al., 1999) and CoREST at the C-terminal (Ballas and Mandel, 2005). In turn, CoREST recruits the histone deacetylase

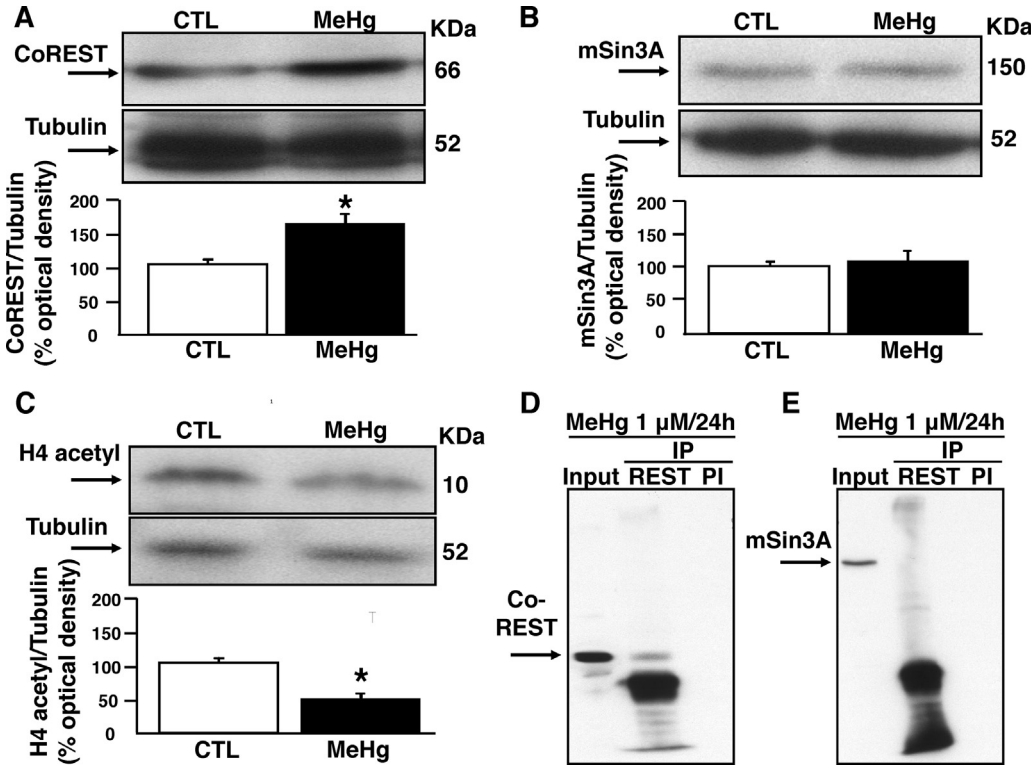

Fig. 3. MeHg elicits REST protein interaction with its cofactor CoREST, but not with mSIN3A, thereby increasing histone H4 deacetylation in SH-SY5Y cells. (A–C) Representative Western blots of CoREST, mSIN3A, and histone H4 acetylation protein levels in CTL and after 24 h of 1 μM MeHg treatment. Graphs show the quantification of the ratio of CoREST, mSIN3A, and histone H4 acetylation to tubulin. Bars represent mean ± S.E.M. obtained from four independent experimental sessions. $^{*}P < 0.05$ vs. CTL. (D,E) Representative Western blot showing immunoprecipitation between REST and CoREST and between REST and mSIN3A after 24 h of 1 μM MeHg treatment. IgG was used as a negative control.

(HDAC) proteins binding to the promoter sequences of its target genes, determining their repression. Intriguingly, we found that MeHg upregulated CoREST, but not mSin3A, thereby causing a reduction in histone H4 acetylation. Consistently, when we pre-treated cells with the HDAC inhibitor TSA, MeHg-induced H4 deacetylation was significantly blocked, thereby reverting the neurotoxicity of MeHg and the cleavage of caspase 3. Since deacetylation of both H3 and H4 histones is used as marker of REST target gene transcriptional repression (Calderone et al., 2003b, Formisano et al., 2007, Noh et al., 2012), we could hypothesize that also histone H3 acetylation is reduced after MeHg treatment. In fact, it has been shown that in cells exposed to other environmental toxicants, like PCBs, REST caused cell death by inducing H3 and H4 histone deacetylation and TSA, by reverting A1254-induced H3 and H4 deacetylation, reduced cell death (Formisano et al., 2011). Furthermore, these results suggest that the REST/CoREST/HDAC pathway—also involved in brain ischemia (Noh et al., 2012)—plays a key role in the mechanisms involved in MeHg-induced neurotoxic effects. Furthermore, since CoREST mediates primarily long-term silencing of target genes, whereas mSin3A mediates dynamic and reversible gene repression (Ballas et al., 2005, Lunyak et al., 2002), we speculate that MeHg, by inducing REST-CoREST interaction, determines a long term silencing of neuroprotective REST target genes, such as NCX1 (Formisano et al., 2013), GriA2 (Calderone et al., 2003a), and Synapsin-1 (Formisano et al., 2011). Regarding the MeHg concentrations, it should be underlined that we used the same MeHg doses as those used by other authors in the same cell line, (Ndountse and Chan, 2008, Toyama et al., 2010), *i.e.*, with an IC50 approximately of 0.5 and 1 μM.

The most meaningful result of this paper is that MeHg-induced REST increase caused an apoptotic cell death; whereas it was previously reported that the REST increase induced by exposure to other environmental toxicants determined a necrotic cell death in SH-SY5Y cells (Formisano et al., 2011, Formisano et al., 2014, Formisano et al., 2015a, Guida et al., 2015). This discrepancy in the kind of REST-induced cell death could be due to the difference in REST cofactors CoREST and mSIN3A recruitment. Indeed, MeHg induced the recruitment of CoREST only, whereas PCB exposure induced the recruitment of both cofactors CoREST and mSin3A. The results of the present study are in accordance with Noh et al., 2012, where global brain ischemia, that is known to determine apoptotic cell death in CA1 neurons (Abe et al., 1995, Jover-Mengual et al., 2010, Ni et al., 1998), increases REST and CoREST, but not mSin3A (Noh et al., 2012).

Given that the cerebellum is the best-characterized target of MeHg toxicity both in humans and rodents (Eto et al., 2010; Nagashima, 1997), we examined REST expression in the cortex and cerebellum of mice treated with MeHg.

As regards the dose of MeHg used in our *in vivo* experiments (10 mg/Kg/day s.c.), it should be considered that the World Health Organization (WHO) and Environmental Protection Agency (EPA) reference dose for hair Hg is now less than 2 ppm, that is 1.8 to 1.2 ppm, respectively, which corresponds to 4,5 and 3 mg/70 kg (0.063 and 0.043 mg/Kg), respectively. Thus, the dose of MeHg used in this work can be considered quite high referring to humans. However, the dose of 10 mg/Kg of MeHg is comparable to that used in rodent studies on the effects of MeHg on Central nervous System (CNS). In fact, it has been shown that this dose is able to elicit a neurological phenotype in adult mice (Dietrich et al., 2005, Farina et al., 2011, Zimmermann et al., 2014). In addition, *s.c.* injection of 10 mg/Kg of MeHg has been used to demonstrate that L-Met enhances cerebellar deposition of Hg in mice exposed to the

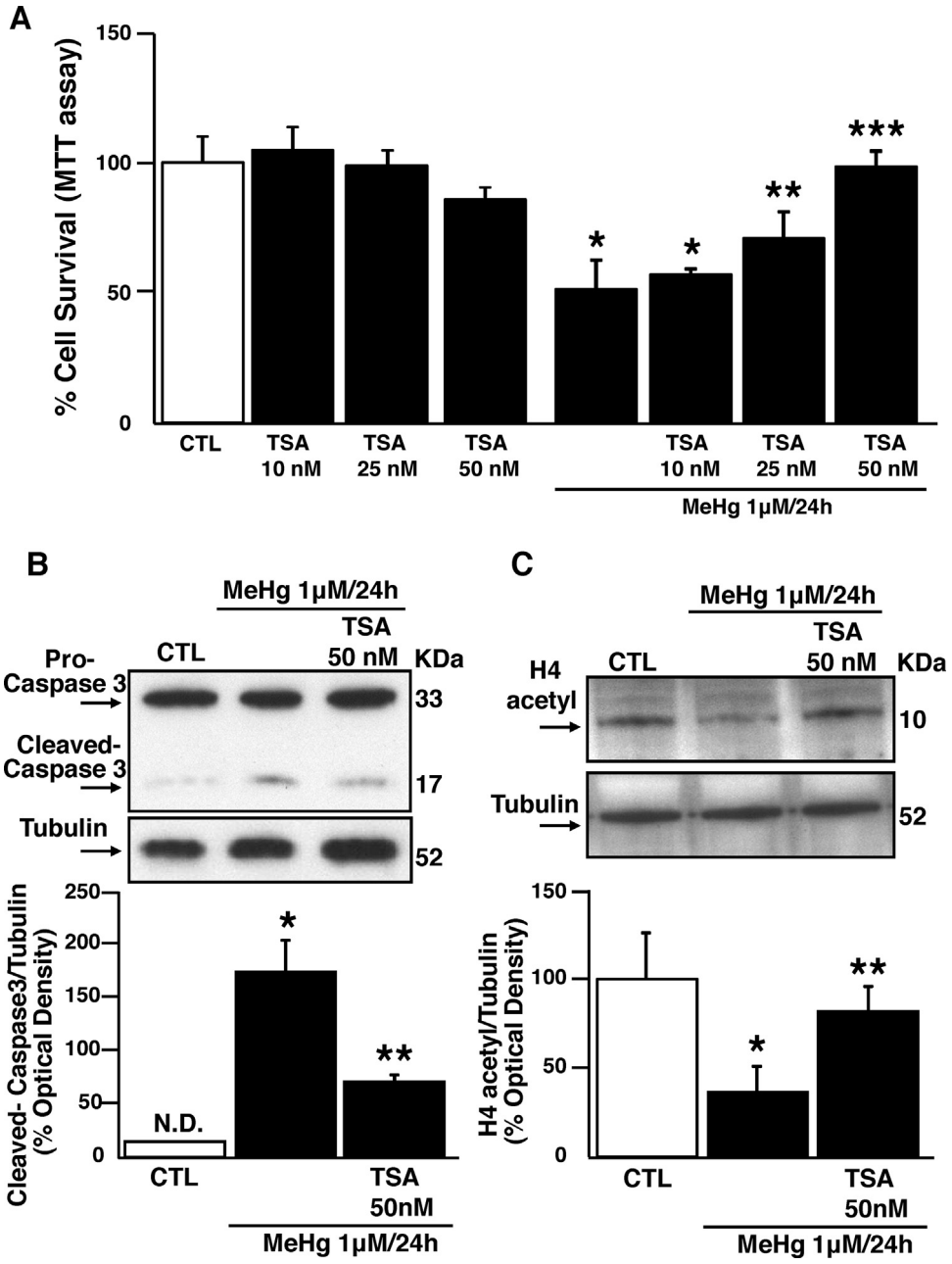

Fig. 4. Effect of pan HDAC inhibitor TSA on MeHg-induced apoptosis in SH-SY5Y cells.
(A) Effect of 24 h MeHg (1 μM) exposure alone or after pretreatment with TSA on MTT at 10, 25 and 50 nM. Bars represent mean ± S.E.M. obtained from four independent experimental sessions. $^{*}P < 0.05$ vs. CTL 1, $^{**}P < 0.05$ vs. MeHg (1 μM) and MeHg (1 μM) + TSA (10 nM); $^{***}P < 0.05$ vs. all. (B,C) Representative Western blots of pro-caspase-3, cleaved caspase-3, and tubulin levels in CTL or after a 24 h exposure to 1 μM MeHg, alone or after 2 h pretreatment with TSA (50 nM). Graphs show the quantification of the ratio of cleaved caspase-3 or H4 to tubulin. Bars represent mean ± S.E.M. obtained from three independent experimental sessions. $^{*}P < 0.05$ vs. CTL; $^{**}P < 0.05$ vs. 1 μM MeHg; N.D. not detectable.

toxicant, and that this higher deposition may be responsible for the greater motor impairment observed in mice simultaneously exposed to MeHg and L-Met (Zimmermann et al., 2014).

In this study we found that MeHg treatment (10 mg/kg) increased REST protein expression and decreased histone H4 acetylation in the cerebellum, but not in the cortex. Moreover, IHS analysis revealed that REST was basally expressed in the granular and molecular cell layers, whereas it was very low in the Purkinje cells. The increase in REST and the decrease in histone H4 acetylation occurred in the regions of the cerebellum that are most vulnerable to MeHg intoxication. Consistently, studies show that MeHg induces specific degeneration of the granule cell layers but not of Purkinje cells (Nagashima et al., 1996).

Collectively, these findings document that MeHg induces apoptotic cell death by increasing REST expression in SH-SY5Y cells. REST, in turn, interacts with CoREST, which by recruiting HDACs on the REST target genes promoter, determines a subsequent decrease in histone H4 acetylation. Equally revealing is having evidenced for the first time that MeHg increases REST expression specifically in mice cerebellum granular neurons—thereby making REST a possible new molecular target in the pathogenesis of cerebellar disorders due to MeHg intoxication.

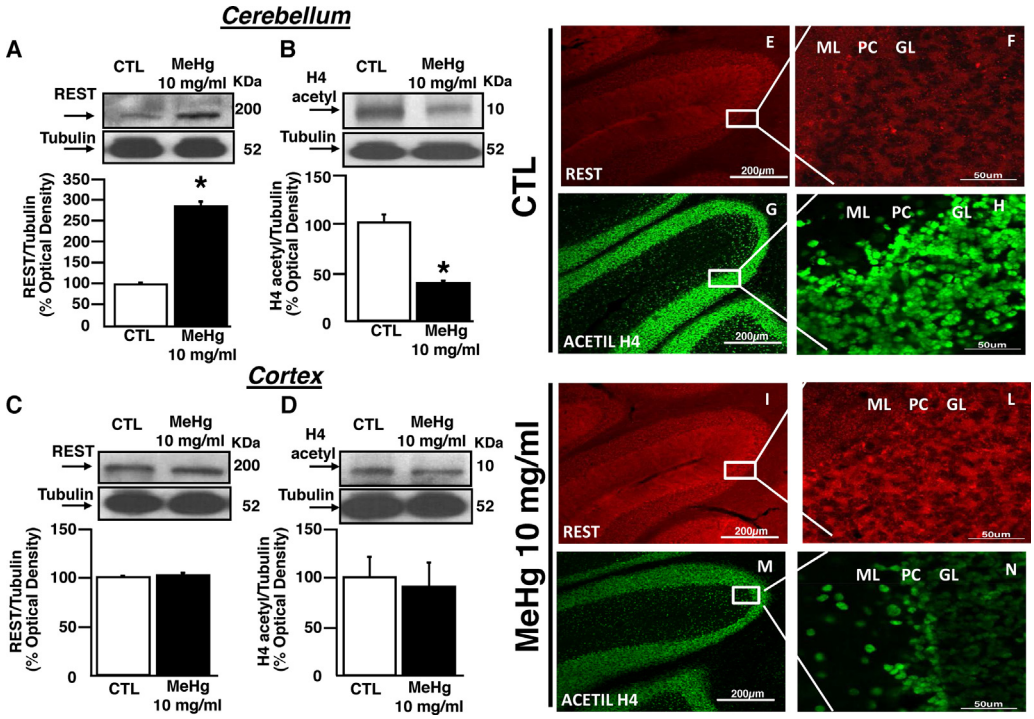

Fig. 5. Effect of MeHg on REST and H4 histone acetylation expression in mouse cerebellum
(A–D) Representative Western Blots of REST and acetylated histone H4 and tubulin in control mice (CTL) and in mice subcutaneously-injected with MeHg (10 mg/Kg) once a day for 10 days. Graphs show quantification of the ratio of REST and acetylated histone H4 to tubulin in cerebellum (A,B) and cortex (C,D). Bars represent mean ± S.E.M. obtained from four independent experimental sessions. $^{*}P < 0.05$ vs. CTL. E-N) Fluorescence images showing REST (red) and H4 histone acetylation (green) immunosignals in cerebellar cortical layers of mice receiving control vehicle (CTL) (E–H) or MeHg (10 mg/Kg) (I–N) for 10 days. (F, H) Higher magnification of the frame depicted in E and G displaying REST and H4 histone acetylation immunoreactivity in control group (CTL). (L,N) Higher magnification of the frame depicted in I and M displaying REST and H4 histone acetylation immunoreactivity in MeHg-treated mice. Scale bars in E, G, I and, M is 200 μm; in F, H, L and N 50 μm. Abbreviations: ML, molecular layer, PC, Purkinje cells and GL, granular layer.

5. Conflict of interest

The authors declare no conflicts of interest.

Acknowledgements

The authors also thank Carmine Capitale for technical support and Dr. Paola Merolla for stylistic editing. This work was supported by grants: from [COFIN2008], Ricerca finalizzata [2009] PON 01_01602 and PON 03PE_00146_1 to Lucio Annunziato. POR Campania FESR 2007-2013 OCKEY (B25C13000280007) to Gianfranco.Di .Renzo.

References

Abe, K., Aoki, M., Kawagoe, J., Yoshida, T., Hattori, A., Kogure, K., et al., 1995. Ischemic delayed neuronal death. A mitochondrial hypothesis. Stroke 26, 1478–1489.

Bal-Price, A., Brown, G.C., 2000. Nitric-oxide-induced necrosis and apoptosis in PC12 cells mediated by mitochondria. J. Neurochem. 75, 1455–1464.

Ballas, N., Grunseich, C., Lu, D., Speh, J., Mandel, G., 2005. REST and its corepressors mediate plasticity of neuronal gene chromatin throughout neurogenesis. Cell 121, 645–657.

Ballas, N., Mandel, G., 2005. The many faces of REST oversee epigenetic programming of neuronal genes. Curr. Opin. Neurobiol. 15, 500–506.

Calderone, A., Jover, T., Noh, K., Tanaka, H., Yokota, H., Lin, Y., et al., 2003a. Ischemic insults derepress the gene silencer REST in neurons destined to die. J. Neurosci. 23, 2112–2121.

Calderone, A., Jover, T., Noh, K.M., Tanaka, H., Yokota, H., Lin, Y., et al., 2003b. Ischemic insults derepress the gene silencer REST in neurons destined to die. J. Neurosci. 23, 2112–2121.

Dietrich, M.O., Mantese, C.E., Anjos, G.D., Souza, D.O., Farina, M., 2005. Motor impairment induced by oral exposure to methylmercury in adult mice. Environ. Toxicol. Pharmacol. 19, 169–175.

Eto, K., Marumoto, M., Takeya, M., 2010. The pathology of methylmercury poisoning (Minamata disease): The 50th Anniversary of Japanese Society of Neuropathology. Neuropathology 30, 471–479.

Fahrion, J.K., Komuro, Y., Li, Y., Ohno, N., Littner, Y., Raoult, E., et al., 2012. Rescue of neuronal migration deficits in a mouse model of fetal Minamata disease by increasing neuronal Ca2 + spike frequency. Proc. Natl. Acad. Sci. USA 109, 5057–5062.

Farina, M., Rocha, J.B., Aschner, M., 2011. Mechanisms of methylmercury-induced neurotoxicity: evidence from experimental studies. Life Sci. 89, 555–563.

Formisano, L., Guida, N., Cocco, S., Secondo, A., Sirabella, R., Ulianich, L., et al., 2011. The repressor element 1-silencing transcription factor is a novel molecular target for the neurotoxic effect of the polychlorinated biphenyl mixture aroclor 1254 in neuroblastoma SH-SY5Y cells. J. Pharmacol. Exp. Ther. 338, 997–1003.

Formisano, L., Guida, N., Laudati, G., Boscia, F., Esposito, A., Secondo, A., et al., 2014. Extracellular signal-related kinase 2/specificity protein 1/specificity protein 3/repressor element-1 silencing transcription factor pathway is involved in Aroclor 1254-induced toxicity in SH-SY5Y neuronal cells. J. Neurosci. Res..

Formisano, L., Guida, N., Laudati, G., Mascolo, L., Di Renzo, G., Canzoniero, L.M., 2015a. MS-275 Inhibits Aroclor 1254-Induced SH-SY5Y Neuronal Cell Toxicity by Preventing the Formation of the HDAC3/REST Complex on the Synapsin-1 Promoter. J. Pharmacol. Exp. Ther. 352, 236–243.

Formisano, L., Guida, N., Valsecchi, V., Cantile, M., Cuomo, O., Vinciguerra, A., et al., 2015b. Sp3/REST/HDAC1/HDAC2 Complex Represses and Sp1/HIF-1/p300 Complex Activates ncx1 Gene Transcription, in Brain Ischemia and in Ischemic Brain Preconditioning, by Epigenetic Mechanism. J. Neurosci. 35, 7332–7348.

Formisano, L., Guida, N., Valsecchi, V., Pignataro, G., Vinciguerra, A., Pannaccione, A., et al., 2013. NCX1 is a new rest target gene: role in cerebral ischemia. Neurobiol. Dis. 50, 76–85.

Formisano, L., Noh, K., Miyawaki, T., Mashiko, T., Bennett, M., Zukin, R., 2007. Ischemic insults promote epigenetic reprogramming of mu opioid receptor expression in hippocampal neurons. Proc. Natl. Acad. Sci. USA 104, 4170–4175.

Fujimura, M., Usuki, F., 2014. Low in situ expression of antioxidative enzymes in rat cerebellar granular cells susceptible to methylmercury. Arch. Toxicol. 88, 109–113.

Fujimura, M., Usuki, F., 2015. Methylmercury causes neuronal cell death through the suppression of the TrkA pathway: in vitro and in vivo effects of TrkA pathway activators. Toxicol. Appl. Pharmacol. 282, 259–266.

Fujimura, M., Usuki, F., Kawamura, M., Izumo, S., 2011. Inhibition of the Rho/ROCK pathway prevents neuronal degeneration in vitro and in vivo following methylmercury exposure. Toxicol. Appl. Pharmacol. 250, 1–9.

Gasso, S., Cristofol, R.M., Selema, G., Rosa, R., Rodriguez-Farre, E., Sanfeliu, C., 2001. Antioxidant compounds and Ca(2 +) pathway blockers differentially protect against methylmercury and mercuric chloride neurotoxicity. J. Neurosci. Res. 66, 135–145.

Guida, N., Laudati, G., Anzilotti, S., Secondo, A., Montuori, P., Di Renzo, G., et al., 2015. Resveratrol via sirtuin-1 downregulates RE1-silencing transcription factor (REST) expression preventing PCB-95-induced neuronal cell death. Toxicol. Appl. Pharmacol..

Guida, N., Laudati, G., Galgani, M., Santopaolo, M., Montuori, P., Triassi, M., et al., 2014. Histone deacetylase 4 promotes ubiquitin-dependent proteasomal degradation of Sp3 in SH-SY5Y cells treated with di(2-ethylhexyl)phthalate (DEHP), determining neuronal death. Toxicol. Appl. Pharmacol..

Huang, Y., Myers, S.J., Dingledine, R., 1999. Transcriptional repression by REST: recruitment of Sin3A and histone deacetylase to neuronal genes. Nat. Neurosci. 2, 867–872.

Hwang, J.Y., Kaneko, N., Noh, K.M., Pontarelli, F., Zukin, R.S., 2014. The gene silencing transcription factor REST represses miR-132 expression in hippocampal neurons destined to die. J. Mol. Biol. 426, 3454–3466.

Jover-Mengual, T., Miyawaki, T., Latuszek, A., Alborch, E., Zukin, R.S., Etgen, A.M., 2010. Acute estradiol protects CA1 neurons from ischemia-induced apoptotic cell death via the PI3K/Akt pathway. Brain Res. 1321, 1–12.

Kaneko, N., Hwang, J.Y., Gertner, M., Pontarelli, F., Zukin, R.S., 2014. Casein Kinase 1 Suppresses Activation of REST in Insulted Hippocampal Neurons and Halts Ischemia-Induced Neuronal Death. J. Neurosci. 34, 6030–6039.

Kazantsev, A.G., Thompson, L.M., 2008. Therapeutic application of histone deacetylase inhibitors for central nervous system disorders. Nat. Rev. Drug Discov. 7, 854–868.

Levenson, J.M., Sweatt, J.D., 2005. Epigenetic mechanisms in memory formation. Nat. Rev. Neurosci. 6, 108–118.

Lunyak, V.V., Burgess, R., Prefontaine, G.G., Nelson, C., Sze, S.H., Chenoweth, J., et al., 2002. Corepressor-dependent silencing of chromosomal regions encoding neuronal genes. Science 298, 1747–1752.

Martin, S.J., Reutelingsperger, C.P., McGahon, A.J., Rader, J.A., van Schie, R.C., LaFace, D.M., et al., 1995. Early redistribution of plasma membrane phosphatidylserine is a general feature of apoptosis regardless of the initiating stimulus: inhibition by overexpression of Bcl-2 and Abl. J. Exp. Med. 182, 1545–1556.

McClelland, S., Brennan, G.P., Dubé, C., Rajpara, S., Iyer, S., Richichi, C., et al., 2014. The transcription factor NRSF contributes to epileptogenesis by selective repression of a subset of target genes. Elife 3, e01267.

Nagashima, K., 1997. A review of experimental methylmercury toxicity in rats: neuropathology and evidence for apoptosis. Toxicol. Pathol. 25, 624–631.

Nagashima, K., Fujii, Y., Tsukamoto, T., Nukuzuma, S., Satoh, M., Fujita, M., et al., 1996. Apoptotic process of cerebellar degeneration in experimental methylmercury intoxication of rats. Acta Neuropathol. 91, 72–77.

Ndountse, L.T., Chan, H.M., 2008. Methylmercury increases N-methyl-D-aspartate receptors on human SH-SY 5Y neuroblastoma cells leading to neurotoxicity. Toxicology 249, 251–255.

Ni, B., Wu, X., Su, Y., Stephenson, D., Smalstig, E.B., Clemens, J., et al., 1998. Transient global forebrain ischemia induces a prolonged expression of the caspase-3 mRNA in rat hippocampal CA1 pyramidal neurons. J. Cereb. Blood Flow Metab. 18, 248–256.

Ninomiya, T., Ohmori, H., Hashimoto, K., Tsuruta, K., Ekino, S., 1995. Expansion of methylmercury poisoning outside of Minamata: an epidemiological study on chronic methylmercury poisoning outside of Minamata. Environ. Res. 70, 47–50.

Noh, K.M., Hwang, J.Y., Follenzi, A., Athanasiadou, R., Miyawaki, T., Greally, J.M., et al., 2012. Repressor element-1 silencing transcription factor (REST)-dependent epigenetic remodeling is critical to ischemia-induced neuronal death. Proc. Natl. Acad. Sci. USA 109, E962–E971.

Olivieri, G., Novakovic, M., Savaskan, E., Meier, F., Baysang, G., Brockhaus, M., et al., 2002. The effects of beta-estradiol on SHSY5Y neuroblastoma cells during heavy metal induced oxidative stress, neurotoxicity and beta-amyloid secretion. Neuroscience 113, 849–855.

Roos, D.H., Puntel, R.L., Farina, M., Aschner, M., Bohrer, D., Rocha, J.B.T., et al., 2011. Modulation of methylmercury uptake by methionine: Prevention of mitochondrial dysfunction in rat liver slices by a mimicry mechanism. Toxicol. Appl. Pharmacol. 252, 28–35.

Simmons-Willis, T.A., Koh, A.S., Clarkson, T.W., Ballatori, N., 2002. Transport of a neurotoxicant by molecular mimicry: the methylmercury-L-cysteine complex is a substrate for human L-type large neutral amino acid transporter (LAT) 1 and LAT2. Biochem. J. 367, 239–246.

Toyama, T., Shinkai, Y., Sumi, D., Kumagai, Y., 2010. Carbon monoxide derived from heme oxygenase-2 mediates reduction of methylmercury toxicity in SH-SY5Y cells. Toxicol. Appl. Pharmacol. 249, 86–90.

Uchida, H., Ma, L., Ueda, H., 2010. Epigenetic gene silencing underlies C-fiber dysfunctions in neuropathic pain. J. Neurosci. 30, 4806–4814.

Zimmermann, L.T., dos Santos, D.B., Colle, D., dos Santos, A.A., Hort, M.A., Garcia, S.C., et al., 2014. Methionine stimulates motor impairment and cerebellar mercury deposition in methylmercury-exposed mice. J. Toxicol. Environ. Health A 77, 46–56.

Zuccato, C., Tartari, M., Crotti, A., Goffredo, D., Valenza, M., Conti, L., et al., 2003. Huntingtin interacts with REST/NRSF to modulate the transcription of NRSE-controlled neuronal genes. Nat. Genet. 35, 76–83.